

Thermal shock resistance of laminated ceramic matrix composites

Y. R. WANG, T.-W. CHOU

Center for Composite Materials and Department of Mechanical Engineering, University of Delaware, Newark, DE 19716, USA

The thermal shock resistance capability of laminated ceramic matrix composites is investigated through the study of three-dimensional transient thermal stresses and laminate failure mechanisms. A $(-45^\circ/45^\circ)_s$ SiC/borosilicate glass laminate is utilized as a reference composite system to demonstrate the analytical results. The maximum allowable temperature change, ΔT_{\max} , has been taken as a measure of the thermal shock resistance capability of composites. The effects of fibre orientation, volume fraction, thermal expansion coefficient, Young's modulus, and thermal conductivity on the thermal shock resistance capability, expressed in terms of the maximum allowable temperature change, ΔT_{\max} , have been assessed. Numerical computations are also performed for six composite systems.

1. Introduction

Ceramics and ceramic matrix composites have demonstrated the desirable characteristics of high-temperature strength, and resistance to creep and corrosion. But they also display an unfavourable property, namely, brittleness or notch-sensitivity, which can render such materials highly susceptible to catastrophic failure under thermal shock.

The thermal shock resistance capability of monolithic ceramics has been studied since the 1950s. Cheng [1], in 1951, first demonstrated that the thermal shock resistance of ceramics can be quantified by analysing the nonsteady state thermal stresses in the material. The thermal shock resistance parameter, $R \sim (1 - \nu)\sigma K/\alpha E$, for the ceramics was proposed; where σ is the tensile strength, ν Poisson's ratio, K the thermal conductivity, α the thermal expansion coefficient, and E Young's modulus. Kingery [2] reported in 1955, that the thermal shock resistance capability is not an intrinsic material property, and it depends on the manner in which heat is applied and the geometrical shape of the specimen. Buessem [3] concluded from the experimental investigations that thermal shock tests usually do not lead to useful experimental data. This is because the synergistic effects of all the material properties on the thermal shock resistance, and the influence of a single property cannot be readily quantified from the test data. There is the need of standard tests for identifying the individual material property effects.

More recent interests in thermal shock resistance problems of ceramics and ceramic matrix composites have been developed since 1980. Singh *et al.* [4] first employed heat transfer theory to analyse thermal stress fracture of ceramics subjected to cooling by quenching into fluid media. In addition to specimen size and geometry, and thermal convectivity, the effect

of specimen density on thermal shock resistance was also introduced. Lewis [5] demonstrated the appreciable disagreement between the water-quench thermal shock test data, ΔT_c , and the calculated thermal shock resistance parameter, R . Results showed that the quenching experiments do not appear to be very suitable for a quantitative assessment of thermal shock resistance. Becher *et al.* [6] studied two general thermal shock resistance parameters; one relates the material properties to its resistance to crack initiation under thermal stress and the other relates the properties to the ability of the material to retain its strength in a thermal stress situation where crack initiation is unavoidable. Faber *et al.* [7], in 1981, proposed a novel thermal shock resistance testing and evaluation procedure intended to alleviate the difficulties associated with the variable and very high heat transfer rates and edge effects in testing, and to provide quantitative predictions of thermally induced failure.

Thomas *et al.* and Singh *et al.* [8, 9], in 1981, performed theoretical investigations of thermal shock resistance capability of ceramics induced by convective and radiative heat transfer. Oguma *et al.* [10], in 1986, compared the predicted and experimental behaviour of thermal stress resistance of circular rod specimens of a soda-lime-silica glass and polycrystalline alumina. The comparison indicates that the thermal stress fracture of the specimens is caused by conductive heat transfer. Tiegs and Becher [11] performed the thermal shock testing of an alumina-20 vol% SiC whisker composite. There is no decrease in the composite flexural strength with $\Delta T < 900^\circ\text{C}$, whereas the flexural strength of pure alumina decreases significantly when $\Delta T > 400^\circ\text{C}$. The improvement in performance is due to the increase in fracture toughness due to fibre reinforcement. Orenstein and Green [12] measured the thermal shock resistance of cellular

alumina ceramics by quench tests, with ΔT varied from 22–105 °C. Wang and Chou [13] recently reported an analytical approach for predicting the maximum allowable temperature change when a composite laminate is subjected to sudden heating or cooling.

From a literature review, we find that the area of thermal shock resistance of ceramics and ceramic matrix composites is often one of conflicting results in terms of agreement between the experimental observations and theoretical predictions based upon material parameters. Agreement or disagreement between analytical calculations and experiments may be fortuitous depending upon the particular values estimated for the various properties.

The thermal response of composites is an important consideration not only in their fabrication and processing but also for their durability and long-term performance. However, there is a lack of basic understanding of thermal shock resistance characteristics of anisotropic materials or fibre-reinforced composites in general. This paper is intended to provide some basic understandings of thermal shock resistance capability of fibre-reinforced composite laminates based upon both thermal stress and failure analyses. The thermal shock resistance capability of high-temperature ceramic composites is quantified in terms of the fibre and matrix thermo-elastic and strength properties, fibre volume fraction and fibre orientation. The influence of the fibre orientation angle, thermal expansion coefficient, Young's modulus, and thermal conductivity on the maximum allowable temperature change, ΔT_{\max} , has also been investigated.

2. Thermal shock resistance

2.1. Thermal shock resistance of isotropic materials

The term "thermal shock" on a material implies that it is subjected to a sudden temperature change. Such a temperature change may result in severe thermal stresses and hence cracks in the material. But the rise or fall of temperature in an elastic body does not necessarily result in thermal stresses. If a homogeneous, isotropic and unrestrained elastic body is changed from an initial temperature to a new uniform temperature, there will be no induced thermal stress. On the other hand, if this elastic body is completely restrained from deforming, temperature changes will result in uniform thermal stresses.

An isotropic solid sphere at the initial temperature $T = 0$ and subjected to a thermal environment $T = T_0$ is taken as an example for demonstrating the definition of thermal shock resistance parameter of a material. The thermal stresses induced in the sphere by such a thermal environment are easily obtained as [14]

$$\begin{aligned}\sigma_r &= \frac{2\alpha E}{1-\nu} \left(\frac{1}{r_0^3} \int_0^{r_0} Tr^2 dr - \frac{1}{r^3} \int_0^r Tr^2 dr \right) \\ \sigma_t &= \frac{\alpha E}{1-\nu} \left(\frac{2}{r_0^3} \int_0^{r_0} Tr^2 dr + \frac{1}{r^3} \int_0^r Tr^2 dr - T \right)\end{aligned}\quad (1)$$

where E is Young's modulus, α the coefficient of thermal expansion, ν Poisson's ratio, r_0 the radius of the sphere, T the temperature field, σ_r the radial stress and σ_t the circumferential stress. The equations governing the temperature field for finite heat convection coefficient, h , between the sphere and its environment are [15]

$$\Delta T = \frac{1}{g} \frac{\partial T}{\partial t} \quad (2a)$$

$$-K \left(\frac{\partial T}{\partial r} \right)_{r=r_0} = h[T(r_0, t) - T_0] \quad (2b)$$

where K is the coefficient of heat conduction, g the thermal diffusivity, and t the time.

For a high rate of heat convection between the surface of the sphere and its environment, i.e. h tends to infinity ($T(r_0, t) = T_0$), the thermal stress field induced on the surface of the sphere ($r = r_0$) at the moment of application of the temperature T_0 ($t = 0^+$) is [14]

$$\begin{aligned}\sigma_r &= 0 \\ \sigma_t &= -\frac{E\alpha T_0}{1-\nu}\end{aligned}\quad (3)$$

Kingery [2] introduced the following dimensionless stress parameter

$$\begin{aligned}\sigma^* &= \frac{S}{\sigma_t} \\ &= \frac{S(1-\nu)}{E\alpha T_0}\end{aligned}\quad (4)$$

where S is the tensile strength of the sphere. Then, let

$$\sigma^* = 1 \quad (5)$$

Kingery defined the thermal shock resistance parameter, R , of high rate of heat convection as

$$\begin{aligned}R &= T_0 \\ &= \frac{S(1-\nu)}{E\alpha}\end{aligned}\quad (6)$$

R reflects the range of rapid temperature change which the material can withstand.

For low rate of heat convection between the surface of the sphere and its environment, i.e. h is finite, due to the complexity of the solution of Equations 2a and b, Cheng [1] proposed an approximate relation between σ^* and K

$$\sigma^* = \frac{r_0 h}{3K} \quad (7)$$

Substituting Equation 4 into Equation 7, the thermal shock resistance parameter R for low rate of heat convection is defined as

$$\begin{aligned}R &= \frac{r_0 h T_0}{3} \\ &= \frac{KS(1-\nu)}{E\alpha}\end{aligned}\quad (8)$$

R is proportional to the applied temperature range and is a function of material intrinsic properties.

The above approaches demonstrate that two basic types of information are necessary to assess the material thermal shock resistance capability. The first is the thermal stress analysis, such as Equation 3; the second is the material failure criterion with reliable strength values. The introduction of the dimensionless stress parameter, σ^* , in Equation 4 indicates that the maximum tensile stress failure criterion has been adopted. Thus, the strength as well as thermo-elastic properties of a material are necessary for thermal shock resistance predictions.

2.2. Thermal shock resistance of composite materials

Just as in the case of homogeneous and isotropic materials, the evaluation of thermal shock resistance of composite materials requires the accurate thermal stress analysis. Considerable effort has been made to investigate the steady state and transient thermal stresses of unidirectional and laminated composites [16–19]. It is clear that due to the mathematical complexities, thermal stresses in fibre composites induced by temperature gradients can be expressed in explicit forms only in very limited cases.

The second requirement for determining the thermal shock resistance of composites is the failure analysis. It has been found that the failure of ceramic matrix composites is much more complicated than that of monolithic ceramics [20]. The failure of laminated composites could be classified as intralaminar and interlaminar. A commonly observed failure mode in composites is delamination initiated at geometric boundaries such as voids, microcracks, free edges, ply drop-off, co-cured joints or bolted joints. Delamination by itself cannot lead to final failure, in-plane fracture must occur for the specimen to lose its load-carrying capability.

In order to simplify the analysis of thermal shock resistance of laminated composites, this paper focuses on the failure initiation (first-ply failure) predicted by the failure criteria. The failure development and ultimate fracture are not considered.

The relationship between thermal shock resistance capability and the structural and material characteristics of high-temperature composites cannot be expressed explicitly in a simple form as Equations 6 and 8 for isotropic materials. Therefore, for the purpose of quantitative studies, the maximum allowable temperature change, ΔT_{\max} , without causing failure, has been taken as a measure of thermal shock resistance of fibre composites. The transient thermal stress analysis given previously [19] for laminated composites is utilized.

Two initial failure mechanisms for high-temperature composites are considered in the present analysis: (1) delamination within the boundary layer region due to the concentration of boundary layer stresses, and (2) matrix micro-cracking induced by in-plane tensile stress. The consideration of the first failure mechanism is consistent with findings in [19]. The second failure mechanism is motivated by the low-toughness/high-strength characteristics of

ceramic matrix composites; matrix micro-cracking has been extensively documented in the literature [21–24].

The mathematical forms of the criteria for initial failure corresponding to the above mechanisms are

$$(1) \sigma_z = \text{interlaminar tensile strength} \quad (9)$$

and

$$(2) \sigma_m = \text{matrix micro-cracking yield stress} \quad (10)$$

where σ_z is the laminate boundary layer normal stress in the thickness direction, and σ_m is matrix tensile stress. Thus in the present analysis, the term “failure” is defined by the state of local stress which attends a strength value of the composites.

The stresses close to the laminate boundary display a high concentration, and they may be 5–30 times larger than those away from the boundary (but still within the boundary layer region) as demonstrated in [19]. Thus, for applying the failure criteria, both the average stresses and peak stresses within the boundary layer region are compared with the strength data. This will be explained further later. The matrix micro-cracking strength, σ_{mcy} , is either obtained from the literature or estimated from the following relationship.

$$\sigma_{mcy} = E \varepsilon_{mcy} \quad (11)$$

where ε_{mcy} is the matrix micro-cracking yield strain and E is the composite Young's modulus. The matrix micro-cracking yield strain of ceramic matrix composites usually ranges from 0.1%–0.2% [25]. The other necessary strength data are calculated from the fibre and matrix strength properties by rule-of-mixtures [26].

3. Numerical examples

A four layer $(- \theta/\theta)_s$ SiC/borosilicate glass (BG) laminate is used as a baseline composite system for parametric studies, Fig. 1. The laminate is of thickness $2h$ (20 mm) and width $2b$ (400 mm); it is infinite in extent along the x -direction. The laminate is uniformly heated at time $t = 0^+$ along the surfaces $y = \pm b$. The numerical computations of thermal shock resistance capability are also performed for five other composite systems (Table I). The constituent fibre and matrix thermoelastic properties can be easily found in the literature [19, 25, 26], and the strength data of these fibres and matrices are given in Table I.

The thermally induced inplane stresses (σ_x and σ_y) and interlaminar normal stress (σ_z) of a $(- 45^\circ/45^\circ)_s$ SiC/BG laminate with 30% fibre volume fraction are depicted in Fig. 2. These stresses are within the laminate boundary layer region and calculated from [19]. The shear stresses are much smaller than the normal stresses. Fig. 2 shows the highly localized stress concentrations of σ_x and σ_z . The peak values (at $Y = 1.0$) of σ_x and σ_z are 4.5 and 1.5 MPa, respectively. σ_y tends to zero when approaching the boundary as the stress boundary condition requires, and the maximum value (at $Y = 0.97$) is 0.34 MPa. Because the variation of σ_y within the boundary layer region is mild, and it is much smaller than σ_x , σ_y is neglected in the failure

TABLE I Identification of composite systems

Matrix	Fibre		
	SiC [27] ($\sigma = 3430, \tau = 588$)	T300 [26] ($\sigma = 2156, \tau = 392$)	Alumino-borosilicate [28] ($\sigma = 1725, \tau = 300$)
BG [27] ($\sigma = 98, \tau = 78$)	(11)*	(12)	(13)
LAS [28] ($\sigma = 32, \tau = 25$)	(21)	(22)	(23)

σ , tensile strength or microcracking stress (MPa).

τ , shear strength (MPa).

BG, borosilicate glass; LAS lithium aluminosilicate.

* Numbers in parentheses indicate composite systems to be used in Fig. 6.

analysis in the x - y plane. The "average" values of σ_x and σ_z near the free-edge are also used in the failure analysis in addition to the maximum stresses at $Y = 1.0$.

Because the stresses σ_x and σ_z demonstrate such significant increases within the laminate boundary

layer region, it is meaningful to obtain also the "average" values of these stresses near the laminate free-edge. A parabolic curve which satisfies the stress boundary conditions is utilized to represent the highly concentrated stress distribution in the region $0.97 \leq Y \leq 1.0$. The "average" is defined by equating the areas under the parabolic curve and average stress line. Finally, the average values of stresses σ_x and σ_z within the laminate boundary layer region are obtained as

$$\begin{aligned} \bar{\sigma}_x &= 1.5 \text{ MPa} \\ \bar{\sigma}_z &= 0.5 \text{ MPa} \end{aligned} \quad (12)$$

For the $(-45^\circ/45^\circ)_s$ laminate, the in-plane stresses in the fibre (σ_1) and transverse to the fibre (σ_2) directions are

$$\begin{aligned} \sigma_1 &= \sigma_2 = \frac{\bar{\sigma}_x}{2} \\ &= 0.75 \text{ MPa} \end{aligned} \quad (13)$$

The transverse Young's modulus, E_2 , of the SiC/BG composite can be obtained from the fibre and matrix elastic properties for a given fibre volume fraction [26]

$$\begin{aligned} E_2 &= E_m \left/ \left[1 - V_f^{1/2} \left(1 - \frac{E_m}{E_f} \right) \right] \right. \\ &= 118.8 \text{ GPa} \end{aligned} \quad (14)$$

where $V_f = 0.3$. The matrix microcracking yield stress σ_{mcy} is obtained from Equation 11.

$$\begin{aligned} \sigma_{mcy} &= E_2 \varepsilon_{mcy} \\ &= 118.8-237.6 \text{ MPa} \end{aligned} \quad (15)$$

where $\varepsilon_{mcy} = 0.1\%-0.2\%$ [25]. The stresses demonstrated in Fig. 2 and calculated in Equation 12 are for unit temperature heating ($T = 1^\circ\text{C}$). From [19], the maximum allowable temperature change, ΔT_{max} , is inversely proportional to the thermal stress, and it can be predicted based upon the matrix micro-cracking failure criterion of Equation 10.

$$\begin{aligned} \Delta T_{max} &= \frac{\sigma_{mcy}}{\sigma_2} \\ &= 158 \text{ to } \sim 316^\circ\text{C} \end{aligned} \quad (16)$$

The ΔT_{max} range in Equation 16 corresponds to $\varepsilon_{mcy} = 0.1\%$ to $\sim 0.2\%$. In the following calculations and figures, $\varepsilon_{mcy} = 0.1\%$ is used when applying the matrix

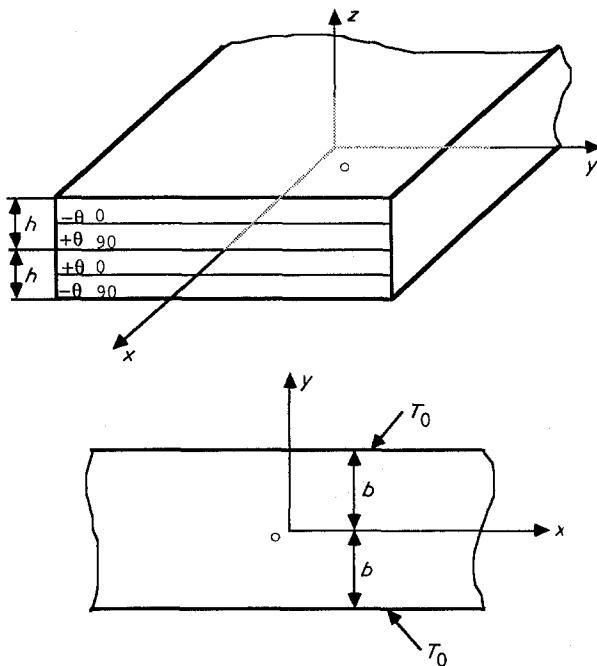


Figure 1 Geometric and thermal boundary conditions of the analytical model.

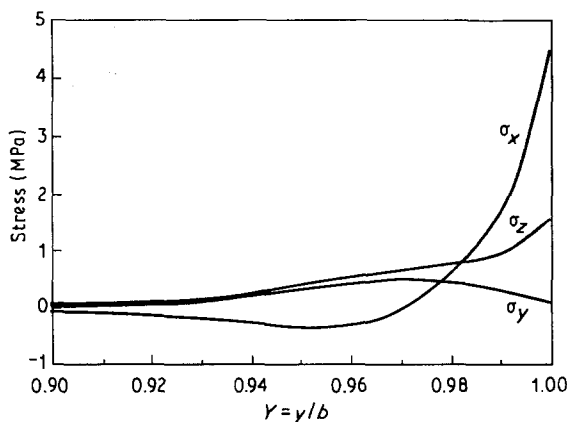


Figure 2 Stress distribution within the boundary layer region, SiC/BG $(-45^\circ/45^\circ)_s$ laminate, $V_f = 30\%$ and $t = 2$ min.

micro-cracking failure criterion. Similarly, the interlaminar strength, σ_{int} , is calculated to be 78 MPa from the literature [19, 26]. Thus, the maximum allowable temperature change, ΔT_{max} , based upon the interlaminar failure criterion is

$$\begin{aligned}\Delta T_{max} &= \frac{\sigma_{int}}{\sigma_z} \\ &= 156^\circ\text{C}\end{aligned}\quad (17)$$

Furthermore, ΔT_{max} is around 55°C if σ_z at the most severe point ($Y = 1.0$) is used in the failure analysis.

The variation of the predicted maximum allowable temperature change, ΔT_{max} , with fibre volume fraction is demonstrated in Fig. 3. The upper line is obtained by using the average stresses within the laminate boundary layer region for the failure analysis, and the lower line is from the peak stresses at $Y = 1.0$. As the fibre volume fraction increases, the stiffness of the composite is enhanced and thus, the stresses within the laminate boundary layer region increase significantly due to the linear elasticity assumption. Although the ultimate failure strength along the fibre direction is improved with fibre volume fraction [26], the matrix microcracking and interlaminar strengths do not show appreciable changes. Therefore, ΔT_{max} is reduced as the fibre volume fraction increases.

For $(-\theta/\theta)_s$ laminates, the interlaminar normal stress σ_z decreases as the fibre orientation angle θ deviates from 45° toward 0° or 90° [19]. On the other hand, the in-plane thermal stress perpendicular to the fibre (σ_2) increases as the fibre orientation angle increases. Thus, the probability of interlaminar failure is reduced and the matrix micro-cracking gradually dominates the laminate failure as θ deviates from 45° . Therefore, the thermal shock resistance capability is reduced with the fibre orientation angle, Fig. 4. The "average" value of stress is utilized in the failure analysis.

The effect of Young's modulus ($\Delta E_3/E_3$), thermal expansion coefficient ($\Delta\alpha_3/\alpha_3$) and thermal conductivity ($\Delta K_3/K_3$) on the variation of ΔT_{max} ($\Delta(\Delta T_{max})$) is evaluated by using a $(-45^\circ/45^\circ)_s$ SiC/BG laminate (Fig. 5) as the reference material. The subscript "3" denotes the through-the-thickness properties. Fig. 5 is

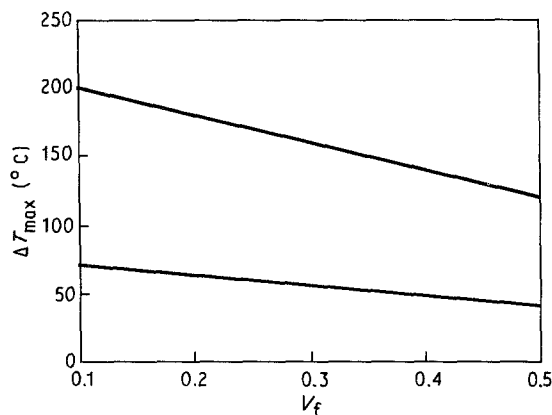


Figure 3 The variation of maximum allowable temperature change, ΔT_{max} , with fibre volume fraction for SiC/BG $(-45^\circ/45^\circ)_s$ laminates.

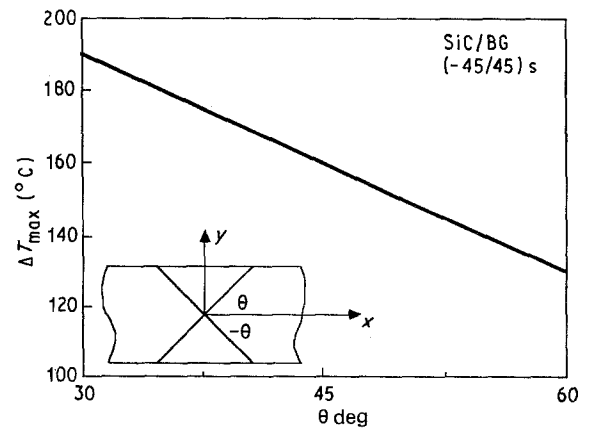


Figure 4 Fibre orientation effect on ΔT_{max} for SiC/BG $(-\theta/\theta)_s$ laminates, $V_f = 30\%$.

calculated by changing one of the properties and keeping other properties constant. The induced thermal stresses vary due to such thermal or elastic property changes. Then, the ΔT_{max} predicted by the above technique also changes due to the variation of thermal stresses. The 40%, 170% and 500% variations in α , E and K , respectively, lead to the same (100%) rise/fall of ΔT_{max} . The trend of the influence of α , E and K on the increase/decrease of ΔT_{max} is similar to that of isotropic material (Equation 8), i.e. R is proportional to K , and inversely proportional to E and α . Fig. 5 is only intended to understand the sensitivity of ΔT_{max} to these material properties and it is understood that the thermo-elastic properties of the SiC/BG system cannot be changed in this manner.

Fig. 6 presents the maximum allowable temperature changes of six composite systems (Table I) with their elastic moduli. The data are generated for $(-45^\circ/45^\circ)_s$ laminates with fibre volume fraction $V_f = 30\%$, and the average stresses are used in the failure analysis. It is found that both delamination and matrix micro-cracking have significant effects. Again, the results presented in this figure are based upon the initial failure only. The composites can still sustain further thermal and mechanical loadings after the initial crack and delamination have formed.

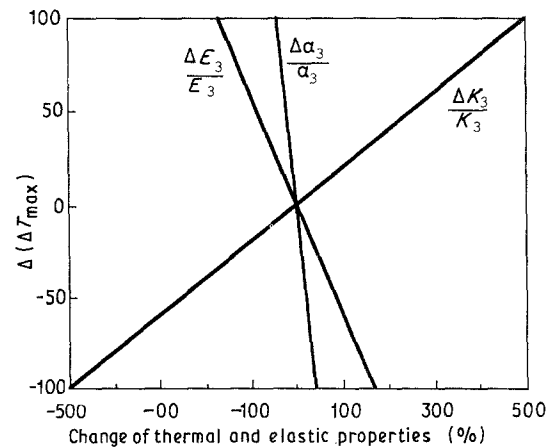


Figure 5 The influence of the per cent changes of $\Delta E_3/E_3$, $\Delta\alpha_3/\alpha_3$ and $\Delta K_3/K_3$ on ΔT_{max} , SiC/BG $(-45^\circ/45^\circ)_s$ laminates, $V_f = 30\%$.

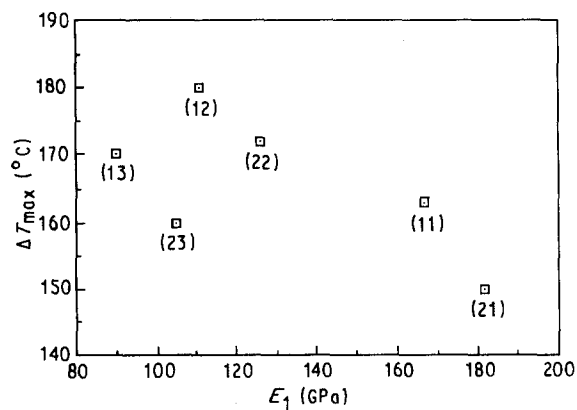


Figure 6 Thermal shock resistance capability, ΔT_{max} , of ($-45^\circ/45^\circ$)_s laminates and composite axial Young's moduli of the six composite systems given in Table I, $V_f = 30\%$.

4. Conclusions

1. The thermal shock resistance parameter of composites cannot be expressed explicitly in a simple form as that for isotropic materials. Therefore, the maximum allowable temperature change, ΔT_{max} , of fibre composites under thermal transient condition without causing failure is adopted as a measure of thermal shock resistance capability.

2. The influence of thermal expansion coefficient, α , Young's modulus, E , and thermal conductivity, K , on thermal shock resistance has been investigated. It is found that change in α has the most effect, while K has the least influence.

3. The initial failure mechanism of ($-\theta/\theta$)_s ceramic matrix composite laminates studied in this paper changes from delamination to matrix microcracking as the fibre orientation angle θ deviates from $\theta = 45^\circ$ toward 0° or 90° .

4. Unlike isotropic materials, fibre composites still maintain their load-carrying capability after the initial failure. Thus, the ultimate failure of the composites does not necessarily occur at temperature changes greater than ΔT_{max} .

Acknowledgement

T. W. Chou acknowledges the support of the Air Force Office of Scientific Research (Contract no. AFOSR-87-0383, Program Manager Dr. Liselotte J. Schioler).

References

1. C. M. CHENG, *J. Amer. Rocket Soc.* **21** (1951) 147.
2. W. D. KINGERY, *J. Amer. Ceram. Soc.* **38** (1955) 3.
3. W. R. BUESSEM, *ibid.* **38** (1955) 15.
4. J. P. SINGH, J. R. THOMAS and D. P. H. HASSELMAN, *ibid.* **63** (1980) 140.
5. D. LEWIS, *ibid.* **63** (1980) 713.
6. P. F. BECHER, D. LEWIS III, W. J. McDONOUGH and R. W. RICE, in "Thermal Stresses in Severe Environments", edited by D. P. H. Hasselman and R. A. Heller (Plenum Press, New York, 1980) pp. 397-411.
7. K. T. FABER, M. D. HUANG and A. G. EVANS, *J. Amer. Ceram. Soc.* **64** (1981) 296.
8. J. R. THOMAS Jr, J. P. SINGH and D. P. H. HASSELMAN, *ibid.* **64** (1981) 163.
9. J. P. SINGH, K. SATYAMURTHY, J. R. THOMAS and D. P. H. HASSELMAN, **64** (1981) 169.
10. M. OGUMA, C. J. FAIRBANKS and D. P. H. HASSELMAN, *ibid.* **69** (1986) C87.
11. T. N. TIEGS and P. F. BECHER, *ibid.* **70** (1987) C109.
12. R. M. ORENSTEIN and D. J. GREEN, in "Ceramic Materials and Components for Engines", edited by V. J. Tennery (American Ceramic Society, Columbus, OH, 1988) pp. 641-50.
13. Y. R. WANG and T. W. CHOU, *ibid.*, pp. 673-82.
14. S. P. TIMOSHENKO and J. N. GOODIER, "Theory of Elasticity", 3rd Edn (McGraw-Hill, New York, 1969).
15. S. KAKAC and Y. YENER, "Heat Conduction" (Hemisphere, Washington, 1985).
16. A. Y. AKOZ and T. R. TAUCHERT, *J. Mech. Engng Sci.* **20** (1978) 65.
17. S. S. WANG and I. CHOI, in "Modern Development in Composite Materials and Structures", edited by J. R. Vinson (ASME, New York, 1979) pp. 315-41.
18. H. S. WANG and T. W. CHOU, *AIAA J.* **24** (1986) 664.
19. *Idem.*, *J. Appl. Mech.* **56** (1989) 601.
20. D. B. MARSHALL and A. G. EVANS, *J. Amer. Ceram. Soc.* **68** (1985) 225.
21. J. AVENSTON, G. A. COOPER and A. KELLY, "Single and Multiple Fracture", Conference Proceedings, National Physical Laboratory, Guildford (IPC Science and Technology Press, 1971) 15.
22. B. BUDIANSKY, W. J. HUTCHINSON and A. G. EVANS, *J. Mech. Phys. Solids* **34** (1986) 167.
23. D. B. MARSHALL, B. N. COX and A. G. EVANS, *Acta Metall.* **33** (1985) 2013.
24. L. N. McCARTNEY, *Proc. Roy. Soc. Lond.* **A409** (1987) 329.
25. T. MAH, M. G. MENDIRATTA, A. P. KATZ, R. RUH and K. S. MAZDIYASNI, *J. Amer. Ceram. Soc.* **68** (1985) 127.
26. C. C. CHAMIS, *SAMPE Q.*, April **15** (1984) 41.
27. T. W. CHOU and J. M. YANG, *Metall. Trans.* **17A** (1986) 1547.
28. K. M. PREWO, J. J. BRENNAN and G. K. LAYDEN, *Ceram. Bull.* **65** (1986) 305.

Received 15 March

and accepted 4 September 1990